Author Manuscript

Author Manuscript

Author Manuscript

Author Manuscript

HHS Public Access

Author manuscript

J Mol Cell Cardiol. Author manuscript; available in PMC 2020 August 13.

Published in final edited form as:

J Mol Cell Cardiol. 2019 January ; 126: 50–59. doi:10.1016/j.yjmcc.2018.11.006.

The SCFFBXO3 ubiquitin E3 ligase regulates inflammation in atherosclerosis

Divay Chandra[a], **James Londino**[a], **Shaun Alexander**[a], **Joseph S. Bednash**[a], **Yingze Zhang**[a], **Robert M. Friedlander**[b], **Grant Daskivich**[a], **Diane L. Carlisle**[b], **William R. Lariviere**[b], **Ana Carolina Igami Nakassa**[b], **Mark Ross**[c], **Claudette Croix St.**[c,d], **Toru Nyunoya**[a,f], **Frank Sciurba**[a], **Bill Chen**[a], **Rama K. Mallampalli**[a,d,e,f,*]

[a]Department of Medicine, University of Pittsburgh, Pittsburgh, PA, United States

[b]Department of Neurological Surgery, University of Pittsburgh, Pittsburgh, PA, United States

[c]Center for Biologic Imaging, University of Pittsburgh, Pittsburgh, PA, United States

[d]Department of Cell Biology, University of Pittsburgh, Pittsburgh, PA, United States

[e]Department of Bioengineering, University of Pittsburgh, Pittsburgh, PA, United States

[f]Medical Specialty Service Line, Veterans Affairs Pittsburgh Healthcare System, Pittsburgh, PA, United States

Abstract

Inflammation is critical in the pathobiology of atherosclerosis. An essential player in the inflammatory process in atherosclerosis are macrophages that scavenge oxidatively modified low-density lipoproteins (OxLDL) deposited in the subendothelium of systemic arteries that secrete a myriad of pro-inflammatory mediators. Here, we identified that a subunit of the Skp-Cullin-F-box ubiquitin E3 ligase apparatus, termed FBXO3, modulates the inflammatory response in atherosclerosis. Specifically, individuals with a hypofunctioning genetic variant of *FBXO3* develop less atherosclerosis. FBXO3 protein is present in cells of monocytic lineage within carotid plaques and its levels increase in those with symptomatic compared with asymptomatic atherosclerosis. Further, cellular depletion or small molecule inhibition of FBXO3 significantly reduced the inflammatory response to OxLDL by macrophages without altering OxLDL uptake. Thus, FBXO3 potentiates vascular inflammation and atherosclerosis that can be effectively mitigated by a small molecule inhibitor.

Keywords

Atherosclerosis; Oxidized low-density lipoprotein; Vascular inflammation; E3 ubiquitin ligase

[*]Corresponding author at: UPMC Montefiore, NW 628, Pittsburgh, PA 15213, United States. mallampallirk@upmc.edu (R.K. Mallampalli).

Disclosures

R.K. Mallampalli and Bill Chen are consultants for *Koutif Therapeutics*, Inc. The other authors declare that they have no conflicts of interest with the contents of this article.

Appendix A. Supplementary data

Supplementary data to this article can be found online at https://doi.org/10.1016/j.yjmcc.2018.11.006.

Author Manuscript Author Manuscript Author Manuscript Author Manuscript

1. Introduction

Atherosclerosis is the number one cause of death in the United States and among the leading causes of morbidity and mortality globally [1]. Inflammation is critical in all stages of atherosclerosis from the formation of a plaque in the vessel wall to its eventual rupture resulting in coronary ischemia, stroke, or peripheral arterial occlusion [2–5]. Therapies that lower circulating low-density lipoprotein (LDL) levels form the cornerstone of atherosclerosis treatment. However, as inflammation has been increasingly implicated in the pathogenesis of atherosclerosis, a new genus of anti-inflammatory therapies has emerged that may provide additional therapeutic benefit beyond LDL reduction [2]. One such anti-inflammatory agent is Canakinumab, a monoclonal antibody that targets interleukin-1β. In a recent clinical trial patients already treated with LDL lowering agents experienced a 15% reduction in recurrent cardiovascular events without any change in circulating LDL levels when administered Canakinumab rather than placebo, providing proof-of-concept and validation of targeted anti-inflammatory therapies for atherosclerosis [6,7]. Because agents like Canakinumab work independent of LDL levels they have the potential to add a new dimension to the treatment of atherosclerosis beyond LDL reduction. These developments underscore the critical need for further investigation of the modulators of the inflammatory response in atherosclerosis and how they can be targeted by novel anti-inflammatory agents [7].

A key inciting event in atherosclerosis is the deposition of circulating low-density lipoprotein (LDL) in the subendothelial space of major arteries. In the subendothelium, native LDL is no longer protected by circulating antioxidants and is oxidatively modified to oxidized LDL (OxLDL) [5]. OxLDL is no longer recognized by the LDL receptor but rather by scavenger receptors such as CD36 on the surface of the macrophage [5]. Once ligated by OxLDL, CD36 recruits Toll-like receptors (TLR) 4 and 6 and activates an intracellular signaling cascade that requires adapter proteins including tumor necrosis factor receptor associated factors (TRAFs) [8,9]. This signaling cascade phosphorylates and activates the p65 subunit of NF-κB resulting in secretion of pro-inflammatory mediators that perpetuate the inflammatory response and establish the atherosclerotic lesion in the vessel wall [8]. Hence, surface receptor activation coupled to signal transduction through key intermediates that stimulate the cytokine response is critical in mediating actions of modified LDL.

It has been shown that the protein stability of TLRs and signaling intermediates such as TRAF proteins are important in controlling pro-inflammatory responses [10]. Ubiquitination controls the lifespan of the majority of proteins and involves a hierarchical, exquisite system. Ubiquitination involves the stepwise transfer of ubiquitin from an E1 ubiquitin-activating enzyme to an E2 ubiquitin-conjugating enzyme, and finally to an E3 ubiquitin ligase complex [11]. In the final step of the reaction, the E3 ubiquitin ligase transfers ubiquitin chains to the substrate to facilitate degradation by the 26S proteasome or sorting to the endosome-lysosome pathway. Two E1 enzymes, almost 40 E2 enzymes, and > 1000 E3 enzymes have been identified in mammalian cells [12]. The Skp-Cullin-F-box (SCF) superfamily represents the largest group of E3 ligases that mediate critical roles in cell biology, including tumorigenesis and inflammation. Within the SCF apparatus is a receptor module, termed F-box protein that binds substrates. We previously identified and

Author Manuscript Author Manuscript Author Manuscript Author Manuscript

characterized the molecular behavior of F-box protein FBXO3, that targets another F-box subunit, FBXL2, that in turn controls the stability of TRAF proteins [10]. Therefore, inhibition of FBXO3 increases FBXL2 which decreases levels of TRAF proteins to limit inflammation. TRAF proteins also link cell-surface receptors such as CD36 to NF-κB which appears to be controlled, in part, by the SCF^{FBXO3} E3 ligase [10]. FBXO3 is a particularly attractive drug target in atherosclerosis because a small molecule inhibitor of FBXO3 is effective in preclinical studies [10].

In this study, we implicate SCF^{FBXO3} E3 ligase as a critical modulator of inflammation in atherosclerosis and demonstrate the efficacy of a small molecule FBXO3 inhibitor in suppressing inflammatory responses important in atherosclerosis. Specifically, individuals carrying a hypofunctioning genetic variant of FBXO3 manifest less atherosclerosis. Also, FBXO3 protein levels are increased in atherosclerotic plaques from subjects with symptomatic rather than asymptomatic atherosclerosis. Further, depletion or chemical inhibition of FBXO3 protein abolishes inflammatory responses to OxLDL without altering OxLDL uptake in macrophages. Thus, these studies implicate FBXO3 as a unique, druggable target for anti-inflammatory therapy in atherosclerosis.

2. Materials and methods

2.1. Human cohorts

All human studies were approved by the Internal Review Board at the University of Pittsburgh and all participants provided written informed consent.

2.1.1. SCCOR cohort—Enrollment criteria for the Pittsburgh SCCOR study have been described previously [13]. In brief, participants were 40–79 years old with a minimum 10 pack-years of current or prior smoking, and without prior vascular or cardiac events. Carotid sonography was performed using standardized methods as described previously (GE 9 L probe, 3–10 MHz, GE Healthcare, Tokyo, Japan and GE Vivid 7 Dimension ultrasound, GE Vingmed Ultrasound, Horten, Norway) [14,15]. Plaque was defined per standardized guidelines as a focal structure protruding ≥0.5 mm into the arterial lumen or ≥1.5 times the thickness of the surrounding intima media [14]. Patients were classified as having none (0 plaque), mild (1–3 plaques) or severe (> 3 plaques) carotid atherosclerosis. Coronary artery calcium score was assessed visually using the Weston method in non-EKG gated chest CT scans. Calcium scores from non-EKG gated CT have excellent correlation with scores from EKG gated CT and have been independently validated as predictors of coronary vascular events and mortality by multiple investigators [16–19]. The Weston scoring system has also been validated against the Agatston score (gold standard) by independent investigators, including our group [17,20]. The Weston score ranges from 0 to 12 with higher scores representing an increased amount of coronary artery calcium. Scores were divided into 4 categories due to their skewed distribution (0 = none, 1–3 = mild, 4–7 = moderate, 8–12 = severe) that correspond to the four categories of Agatston scores (0, 1–100, 101–400, > 400) with sensitivity of 100% and specificity > 85% [17].

Current smoking status, pack-years of smoking, and medication use were self-reported. Systolic and diastolic blood pressure were recorded on the day of the study visit.

Author Manuscript Author Manuscript Author Manuscript Author Manuscript

Hypertension was defined as systolic blood pressure ≥ 140 mmHg or diastolic blood pressure ≥ 90 mmHg measured during the study visit, patient report of the diagnosis, or use of an anti-hypertensive medication. Hyperlipidemia and diabetes were defined by use of a lipid-lowering or diabetic medication respectively or patient report of the diagnosis.

2.1.2. Carotid plaque cohort—Carotid plaque tissue was surgically removed for clinical indications in asymptomatic and symptomatic individuals. Patients were classified as symptomatic if they suffered a transient ischemic attack (TIA), transient monocular blindness ipsilateral to the study artery, or minor or non-disabling ipsilateral stroke. Otherwise, patients were classified as asymptomatic. Plaque tissues were immediately flash frozen after removal from the patient. Clinical information was extracted from the medical record by a physician blinded to experimental findings.

2.2. FBXO3 genotyping

FBXO3 genotyping was performed as described before [10]. In brief, an analysis of human SNP database revealed a naturally occurring nonsynonymous C/T polymorphism (rs1402954) in FBXO3 (V221I) in individuals of European descent with an allele frequency of 6.2%. Genomic DNA was extracted from PBMCs followed by genotyping using a specific primer and probe set [10].

2.3. Antibodies and reagents

FBXO3 antibodies were obtained from Santa Cruz Biotechnology and Abcam. Anti-mouse IgG and anti-rabbit IgG were obtained from Bio-Rad. Phos-p38, p38, phos-JNK, JNK, phos-ERK1/2, ERK 1/2, AKT, and phos-AKT1 antibodies were obtained from Santa Cruz Biotechnology. Phos-p65, total p65, CD36, and CD68 antibodies were obtained from Cell Signaling. CD206 and iNOS antibodies were obtained from Abcam. ICAM1 antibody was obtained from Invitrogen. PMA was obtained from Sigma. Halt protease inhibitor cocktail was obtained from Thermo Scientific. Polymyxin B was obtained from Santa Cruz.

At the beginning of the study, we attempted to make an oxidized LDL preparation by incubating native LDL with copper sulfate. However, the inflammatory response to the resulting OxLDL was inhibited by polymyxin B indicating the presence of LPS. Therefore, this OxLDL preparation was not used for any experiments. Instead, highly oxidized low-density lipoprotein and Di labeled highly oxidized low-density lipoprotein was obtained from Kalen Biomedical (Germantown, MD). The oxidized LDL was certified LPS free (< 0.5 EU per mg of protein) and LDL free (> 97% by gel electrophoresis) by the vendor prior to shipment.

To better characterize this OxLDL preparation we assessed the thiobarbituric acid reactive substances (TBARS) concentration (cat no 700870, Cayman Chemical). TBARS are a byproduct of lipid peroxidation and are a commonly reported index of the extent of oxidization of LDL (Fig. e1 A). Also, we compared the electrophoretic mobility of the highly oxidized LDL relative to native and less oxidized forms of LDL (Fig. e1 B–C). Electrophoretic mobility was assessed using the Hydrasys I semi-automated gel electrophoresis system. 10 ul of each lipoprotein preparation (at 1 mg/mL final protein

Author Manuscript Author Manuscript Author Manuscript Author Manuscript

concentration) was loaded in a 0.8% agarose gel and electrophoresed at 15 W at 20 °C until 100 Vh had accumulated (about 30 min). The gel was then dried at 45 °C for 35 min, stained for 15 min with Sudan black, destained by washing with isopropanol twice, dried for 10 min at 60 °C, photographed, and the migration of the bands relative to native LDL measured using Image J (Fig. e1 B–C).

2.4. Immunoblotting

Supernatants were discarded and the cells washed twice with ice cold PBS. Lysis buffer was added (0.5% Triton in PBS with 1× Halt protease inhibitor cocktail) and the lysate mechanically scraped off the bottom of each well. Lysates were sonicated for 15 s on ice, protein concentration measured (DC protein assay, Bio-Rad), and 15–20 μg/lane of lysate were loaded onto 10% stain free SDS-PAGE gels (Bio-Rad). After electrophoresis, the gels were photographed under UV light to image the protein in the gel according to the manufacturer's instructions. After transferred to nitrocellulose membranes (Trans-Blot Turbo, Bio-Rad) the membranes were re-imaged under UV light to confirm complete and even transfer of the protein from the gel. The membranes were then blocked with 3% (*w*/*v*) BSA in TBST (25 mM Tris-HCl, pH 7.4, 137 mM NaCl, and 0.1% Tween 20) for 1 h, and incubated with primary antibodies in 3% (w/v) BSA in TBST at 4 °C overnight or 1–2 h at room temperature. The membranes were then washed at least three times with TBST at 5-min intervals followed by a 1 h incubation with horseradish peroxidase-conjugated secondary antibody (1:2000). The membranes were developed with an enhanced chemiluminescence detection system according to manufacturer's instructions. Densitometry was performed and adjusted to total protein per lane using automated measurement and rolling disk normalization using Image Lab v5.2.1 according to manufacturer instruction (Bio-Rad). Total protein per lane was used to correct for protein loading rather than housekeeping genes (such as β-actin) because independent studies indicate that the total protein method is more accurate [21–23].

2.5. Carotid tissue protein extraction and staining

Plaque tissue was flash frozen in liquid nitrogen in the operating room after removal from the patient. Protein was extracted using standardized methods. Protein concentration measurement was not possible because the high lipid content interfered with absorbance based microplate assays (DC protein assay, Bio-Rad).

Plaque tissue was thawed in 2% paraformaldehyde for 2 h, transferred to 30% sucrose overnight, and then frozen in liquid nitrogen cooled with isopentane. 6 μM sections were placed onto Superfrost Plus Stain Slides. H & E staining was performed and histology of the sections examined by an experienced neuropathologist at the University of Pittsburgh (Julia Kofler). For immunofluorescence staining, sections were blocked with 5% normal donkey serum for 45 mins. After 5 washes with 0.5% BSA, primary antibody was added at 1:50 for FBXO3, 1:100 for CD68, 1:100 for CD206, 1:100 for iNOS, and 1:100 for ICAM1 in 0.5% BSA overnight at 4 °C. Sections were washed with 0.5% BSA and respective secondary antibodies (Jackson Immuno, CY3 711-165-152, CY5 715-605-150) were added for 60 mins in 0.5% BSA. The sections were then washed, stained with Hoechst dye 30 s (Sigma, B-2883, 1 mg/100 mL dH20), and coverslips mounted using gelvatol. After drying overnight

Author Manuscript Author Manuscript Author Manuscript Author Manuscript

the slides were imaged using a Nikon A1 confocal microscope equipped with a 20× (0.95NA) optic and Nikon NIS Elements v4.4.

2.6. Cell culture

THP-1 cells were obtained from ATCC (Manassas, VA, USA) and cultured in RPMI-1640 (Life Technologies, Grand Island, NY) with 10% fetal bovine serum (Gemini, Sacramento, CA, USA), L-glutamine (2 mM), 1× non-essential amino acids, HEPES (10 mM), sodium pyruvate (1 mM), and 1× Penicillin Streptomycin (Life Technologies, Grand Island, NY). The same batch of fetal bovine serum (Lot no A65F82H) was utilized for cell culture during the entire study. Cells were cultured in suspension and passaged twice a week to maintain a concentration between 250,000–1,000,000/mL. A fresh batch of cells was used every 8–10 weeks. Cells were plated in either 6 or 12 well plates at a concentration of 500,000/mL with 30 nM PMA and allowed to differentiate and adhere to the bottom of the well for 48–72 h prior to experimentation.

2.7. RT-PCR

RNA was isolated from cells using RNeasy Mini Kits (Qiagen) per the manufacturer's instructions. Isolated RNAs were immediately converted to cDNA using High Capacity RNA-to-cDNA Kits (Life Technologies, Grand Island, NY) after their concentrations were measured. Real-time PCR assays were performed using SYBR® Select Master Mix for CFX (2×) (Life Technologies, Grand Island, NY) with the C1000 Thermal Cycler (BioRad, Hercules, CA) per manufacturer instructions.

2.8. Gene silencing

Small interfering RNAs (siRNA) for human FBXO3 were purchased from Integrated DNA Technologies (Coralville, Iowa, *FBXO3* dsiRNA 1: design ID hs.Ri.FBXO3.13.1 and *FBXO3* dsiRNA 2: design ID hs.Ri.FBXO3.13.2), along with control/scramble dsiRNA (cat # 51-01-19-09). Cell culture medium was changed to fresh medium without PMA. Scramble or *FBXO3* dsiRNA (final concentration 50 nM) was mixed with transfection buffer and GenMute transfection reagent (SignaGen Labs, Rockville, MD) according to manufacturer instructions and added to respective wells. Medium was changed 6 h later and the cells allowed to rest for 48 h before experimentation.

2.9. Cellular immunofluorescence

THP-1 cells were plated in 12 well plates with sterile cover slips in each well. Cells were incubated with Di labeled OxLDL (cat no 770262, Kalen Biomedical, Germantown, MD) for the stated time points. The cover slips were then removed, the cells washed thrice with PBS, fixed with 2% formaldehyde for 15 mins, stained with DAPI for 30 s, mounted onto glass slides, and imaged using a Nikon ECLIPSE TE 300 confocal microscope.

To assess p65 nuclear translocation THP1 cells were cultured as above on sterile coverslips. 10 μM BC-1215 was added overnight to the indicated wells followed by 100 μg/mL OxLDL in the morning. 45 min later cells were washed with PBS, fixed with 2% paraformaldehyde for 20 min, permeabilized with 0.1% Triton X 100 for 15 mins, blocked with 2% BSA for 45 mins, and incubated with 1:400 p65 antibody. After 1 h the cells were washed and 1:1000

Author Manuscript Author Manuscript Author Manuscript Author Manuscript

goat anti-rabbit Cy5 secondary antibody was added. Finally, the cells were washed with PBS, stained with phalloidin 488 for 20 min, mounted with DAPI containing mounting medium (Fluoroshield from Abcam), and imaged using a Nikon ECLIPSE TE 300 confocal microscope.

2.10. Enzyme-linked immunosorbent assay (ELISA)

IL-1β, TNF-α, and IL-8 ELISA kits were obtained from R & D Biosystems (Minneapolis, MN). Levels of cytokines in THP-1 supernatant and in sera collected from mice were measured per the protocols provided by the manufacturer.

2.11. Flow cytometry

Differentiated THP-1 cells were incubated with 100 μg/mL Di labeled OxLDL for the stated duration. Cells were then detached by the addition of trypsin, washed multiple times, and assessed by flow cytometry performed using a BD ACCURI C6 flow cytometer (San Jose, CA) and the data analyzed using FlowJo (Ashland, OR).

2.12. Statistical analysis

Descriptive statistics were reported with mean ± standard deviation (SD) or standard error (SE) as indicated. Non-parametric methods were used unless stated otherwise. Analyses were performed using STATA v13 (StataCorp, College Station, TX) and GraphPad Prism version 7.0 for Mac OS, (GraphPad Software, La Jolla, CA).

3. Results

3.1. A hypofunctioning genetic variant of FBXO3 is associated with less carotid and coronary atherosclerosis

Individuals of European descent are known to harbor a hypofunctioning genetic variant of FBXO3 (nonsynonymous C/T polymorphism, rs1402954) with an allele frequency of 6.2%. We sought to determine if this genetic variant impacted the risk of atherosclerosis. The 24 individuals who were heterozygous carriers of the hypofunctioning variant had fewer plaques compared with the 122 individuals with wild-type FBXO3 (Fig. 1A–B). In adjusted analyses, those with the hypofunctioning variant were at 62% lower odds of being in a higher category of severity of carotid atherosclerosis compared to those with wide type FBXO3 (odds ratio = 0.38, 95% CI 1.02-6.49, p = 0.04 adjusted for age, gender, body mass index, presence of hypertension, hyperlipidemia, diabetes, systolic and diastolic blood pressure, current smoking, pack-years of smoking, and use of aspirin, statin, and ACE inhibitors). The hypofunctioning genetic variant was also associated with reduced coronary artery calcium scores in a separate group of 161 individuals from the same cohort. Specifically, in adjusted analyses those with the hypofunctioning variant were at 59% lower odds of being in one higher category of severity of coronary artery calcium score compared to those with wild type FBXO3 (odds ratio = 0.41, 95% CI 0.18–0.94, p = 0.03 adjusted for age, gender, body mass index, diabetes, current smoking, pack-years of smoking, and use of aspirin, statin, and ACE inhibitors). Therefore, reduced function of the FBXO3 protein was associated with reduced risk of atherosclerosis independent of established cardiovascular risk factors.

Author Manuscript Author Manuscript Author Manuscript Author Manuscript

3.2. FBXO3 protein is present in carotid plaques and increased in symptomatic atherosclerosis

We sought to determine if FBXO3 protein is expressed in atherosclerotic plaques, hypothesizing that it colocalizes with cells of monocytic lineage where FBXO3 is known to regulate innate immune pathways. Carotid plaque was surgically excised from a 69 year old patient who had experienced a cerebrovascular event and a 68 year old patient with asymptomatic carotid atherosclerosis. Examination of H & E stained sections revealed that the plaques consisted of fibrocalcific tissue at various stages of maturation from loose to densely hyalinized and contained scattered calcification as well as infiltrating inflammatory cells including foamy macrophages (Supplementary Fig. e2).

Immunostaining for FBXO3 demonstrated colocalization with the monocytic lineage marker CD68 in both patients (Fig. 2A–B). Because all CD68 positive cells did not stain for FBXO3, we sought to determine if FBXO3 expression was limited to macrophages demonstrating M1 or M2 polarization. Additional immunostaining for a macrophage M1 marker iNOS and the M2 marker CD206 in combination with CD68 revealed that of the FBXO3 expressing cells that were positive for CD68, 72% ± 13.2% were positive for iNOS and 34.2 ± 19.6% were positive for CD206 (Supplementary Fig. e3). Therefore FBXO3 expression did not appear to be restricted to an M1 or M2 subtype in macrophages in carotid plaques.

Further, to determine if FBXO3 was expressed in endothelial cells, we stained these carotid plaques for ICAM1 (Supplementary Fig. e3). Quantification of the stains suggested that 11.3 ± 8.5% of FBXO3 expressing cells were positive for ICAM-1 while 55.5 ± 27.6% of FBXO3 expressing cells were positive for CD68. Thus, FBXO3 is present in endothelial cells, however, in smaller amounts relative to macrophages.

Protein was then extracted from surgically excised carotid plaques from an additional four individuals with asymptomatic and an additional three individuals with symptomatic carotid atherosclerosis (Fig. 2C) and processed for FBXO3 immunoblotting. There was nearly a 4-fold increase in FBXO3 protein expression in those with symptomatic rather than asymptomatic atherosclerosis (Fig. 2D–E). Thus, these results suggest that FBXO3 protein is present in plaque tissues in cells of monocytic lineage and its levels positively correlate with severity of the disease process.

3.3. FBXO3 depletion does not impact OxLDL uptake

To examine mechanistically how FBXO3 might impact the pathobiology of atherosclerosis, we first examined OxLDL processing within cells of monocytic lineage [10]. In this model, THP-1 monocytes are first differentiated into a macrophage phenotype by incubation with phorbol 12-myristate 13-acetate (PMA) for 48–72 h. After treatment these cells uniformly stained positive for CD68 (Supplementary Fig. e4). Cells were then exposed to OxLDL generated by copper sulfate oxidation of native LDL [24]. The cells recognize OxLDL via the CD36 scavenger receptor on cell membranes leading to TLR4 and TLR6 recruitment triggering internalization of these modified particles [8], NF-κB activation, and secretion of

Author Manuscript Author Manuscript Author Manuscript Author Manuscript

downstream inflammatory mediators (Fig. 3D–H) [8]. The internalization of OxLDL by these cells was concentration and time dependent (Fig. 3A–C).

Using this model, we first determined if altering FBXO3 levels would impact the internalization of OxLDL. FBXO3 protein levels were effectively depleted in THP-1 cells using small interfering RNA to mimic the effects of the hypofunctioning genetic variant of FBXO3 described above (dsiRNA, Fig. e4 B–D). Depletion of FBXO3 protein did not impact the intracellular content of Di labeled OxLDL assessed by flow cytometry at various time points (Fig. 4A–C). Lack of change in OxLDL content with depletion of FBXO3 was confirmed by confocal imaging of the cells (Fig. 4D). Further, protein levels of CD36 at the cell membrane at baseline and in the presence of OxLDL were not altered by FBXO3 depletion (Fig. 4E). CD36 appeared as a dual band in our immunoblots consistent with prior publications [25,26] and likely because it is heavily post-translationally modified by N-linked glycosylation [27]. These studies suggest that FBXO3 does not regulate OxLDL uptake in macrophages.

3.4. FBXO3 depletion in macrophages reduces OxLDL inflammatory responses

Next, we sought to determine if rather than uptake of OxLDL, FBXO3 modulates the inflammatory response to OxLDL. Exposure to OxLDL induced phosphorylation of p65 under basal conditions, however, this phosphorylation was prevented by depletion of FBXO3 (Fig. 5A–B). In contrast, there was no significant change in the level of activation of the p38, JNK, ERK ½, or Akt kinases. Levels of FBXO3 protein were not induced by OxLDL (Fig. 5A). The OxLDL preparation used in this study did not contain detectable levels of LPS per the manufacturer. Further, preincubation of OxLDL with polymyxin B for 60 mins at 37 °C before addition to the cells did not reduce the inflammatory response confirming the absence of LPS in the OxLDL preparation (Fig. 5C). As a biological correlate, these effects of FBXO3 cellular depletion were associated with reduced secretion of pro-inflammatory cytokines IL-1β, IL-8, and TNF-α (Fig. 5D–F). Thus, these cellular in vitro studies suggest a new functional link between FBXO3 and the pro-inflammatory actions of OxLDL.

3.5. A small molecule FBXO3 inhibitor reduces OxLDL inflammatory responses

Results thus far suggest that FBXO3 may represent a unique molecular target to mitigate vascular inflammation driven by modified lipoproteins in macrophages. Therefore, we examined if BC-1215, a small molecule inhibitor of FBXO3, could suppress the inflammatory response to OxLDL in macrophages. Addition of BC-1215 in nanomolar concentrations reduced phosphorylation of p65 and RNA for pro-inflammatory cytokines IL-1β and TNF-α similar to FBXO3 silencing (Fig. 6A–D). BC-1215 also partially attenuated p65 nuclear translocation in the presence of OxLDL (Fig. 6E). Further, treatment with BC-1215 did not impact oxidized LDL uptake similar to FBXO3 silencing (Fig. e5). Therefore, BC-1215 may be a potential anti-inflammatory compound for atherosclerosis suitable for testing in additional preclinical models.

Author Manuscript Author Manuscript Author Manuscript Author Manuscript

4. Discussion

The role of pro-inflammatory pathways linked to the ubiquitin-proteasome system in the pathogenesis of atherosclerosis is an emerging area of investigation. Indeed, studies demonstrate putative roles of proteasomal blockade, protective effects of ubiquitin E3 ligases, and identification of related susceptibility genes, in the pathobiology of atherosclerosis [28]. This study implicates, for the first time, the SCF^{FBXO3} E3 ligase as a unique molecular regulator of inflammation in atherosclerosis. Specifically, we observed that i) individuals carrying a hypofunctioning genetic variant of *FBXO3* manifest less atherosclerosis, ii) FBXO3 protein is present in cells of monocytic lineage within atherosclerotic plaques and its levels are elevated in subjects with symptomatic disease, and iii) FBXO3 inhibition via genetic silencing or chemical inhibition reduces OxLDL induced pro-inflammatory signal events in macrophages. Although additional proof-of-concept studies will be needed, these data suggest that selective FBXO3 targeting might serve as a potentially attractive pharmacotherapeutic strategy in this cardiovascular disorder.

Inflammation is critical in the pathobiology of atherosclerosis. The inflammatory mediators impacted by FBXO3 described herein i.e. NF-κB, IL-1β, and TNF-α, and IL-8 have purported causal roles in atherosclerosis. For example, NF-κB activation is increased in mononuclear cells in human plaques [29] and in peripheral blood mononuclear cells in patients with unstable angina [30], and NF-κB inhibition attenuates atherosclerosis in hyperlipidemic mice [31]. IL-1β is a classic pro-inflammatory cytokine that has been linked to atherosclerosis and has been extensively studied [32]. Antagonizing IL1-β with a monoclonal antibody reduces atherosclerotic events in humans [3]. IL-8 causes rolling monocytes to adhere to endothelial cells, is mitogenic and chemotactic for vascular smooth muscle cells, and is increased within unstable atherosclerotic plaques [33,34]. TNF-α is a potent stimulator of several of the matrix metalloproteinases and of plasminogen activator inhibitor-1 [35] and has been identified as a player in several of the complications of atherosclerosis. Inhibition of TNF-α reduces atherosclerosis in apolipoprotein E knockout mice [35,36]. Hence, NF-κB antagonism, and reduced production of IL1-β, TNF-α, and IL-8 by upstream molecular inputs within the ubiquitin apparatus such as FBXO3 depletion would be expected to impair the development of atherosclerosis.

Our study is not the first to implicate genetic variants in the FBXO3 gene as modulators of atherosclerosis risk. A genome wide association study that included over 5000 African-American participants and examined 2.5 million SNPs identified two variants in FBXO3 (rs11825259 and rs12291756) as among the top 67 SNPs associated with atherosclerosis risk. Unlike the SNP that was genotyped in our cohort, little is known about how rs11825259 and rs12291756 may alter function of FBXO3 [37]. Nonetheless, these independent findings corroborate the potential role of FBXO3 in regulating atherosclerosis in humans.

There are multiple E3 ligases that can impact the pathobiology of atherosclerosis [38,39]. For example, HECT domain E3 ligases HUWE1 and NEDD4–1 control stability of the ATP-binding cassette transporter ABCG1 and ABCG4, both critical for cholesterol homeostasis [40]. In addition, the E3 ubiquitin ligase IDOL triggers lysosomal degradation of the low-

Author Manuscript Author Manuscript Author Manuscript Author Manuscript

density lipoprotein receptor [41]. Also, the ubiquitin ligase von Hippel-Lindau controls stability of hypoxia-inducible factor (HIF)-1a that in turn transcriptionally controls vascular endothelial growth factor (VGEF), an important regulator of neovascularization of atherosclerotic lesions [42]. Further, the E3 ubiquitin ligase ITCH modulates lipid metabolism and atherosclerosis by ubiquitination of SIRT6 and SREBP2, while genetic variants in E3 ligase RNF213 that regulates non-canonical Wnt signaling pathway have been associated with intracranial atherosclerosis [43,44]. While these studies demonstrate how the ubiquitin proteasome system can regulate atherosclerosis, no ubiquitin based therapies for atherosclerosis have been demonstrated as yet, nor have any SCF F-box protein E3 ligases been implicated in atherosclerosis to our knowledge.

Modulating protein stability, specifically inhibiting ubiquitin E3 ligases, provides potential advantages over other druggable targets given the presence of biochemically multiple, unique pharmacophores within complexes that can bind a variety of small molecules [12]. The FBXO3 inhibitors used here were generated using in silico design and have been shown to ameliorate severity of inflammation in several preclinical models of cytokine-driven inflammation [10]. The FBXO3 inhibitor BC-1215 is a tool compound that binds within the ApaG domain of the protein. A Pan labs screen demonstrated that it exhibits 15/109 off-target hits mainly in the serotonin and adrenergic pathways (data not shown). The mechanistic centerpiece for targeting of FBXO3 rests upon its ability to upregulate NF-κB signaling through polyubiquitination and degradation of a constitutively active inhibitor of TRAF proteins, FBXL2 [10]. These results provide relevant pharmacodynamic and pharmacokinetic associations with biologic relevance that validate FBXO3 as a potential therapeutic target in preclinical models.

The current study examines the ability of FBXO3 inhibition to counteract activation of p65 induced by oxidized LDL in macrophages. However, other cell types such as endothelial and smooth muscle cells may also be activated by OxLDL and lesional macrophages may be activated by micro-environmental cues besides OxLDL. We have not as yet demonstrated if FBXO3 inhibition can counteract the effects of OxLDL in other cell types or other pro-inflammatory stimuli to lesional macrophages.

5. Conclusion

This study implicates the SCF E3 ligase FBXO3 in the pathogenesis of atherosclerosis, and demonstrates its potential as a distinct anti-inflammatory therapeutic target. It is likely that other F-box E3 ligases also regulate atherosclerosis. Drugs targeting the ubiquitin proteasome pathway are already being used in the clinical setting to treat cancer and rejection in organ transplantation. Further examination of the benefits of FBXO3 inhibitors in atherosclerosis is warranted.

Supplementary Material

Refer to Web version on PubMed Central for supplementary material.

Author Manuscript Author Manuscript Author Manuscript Author Manuscript

Acknowledgments

We would like to thank Aki Hoji for assistance with interpreting flow cytometry data, Ping An for assistance with RT-PCR, Dr. Julia Kofler for interpretation of H & E stains of carotid plaque, and Kathy K. Foxx (Kalen Biomedical, Germantown, MD) for assistance with characterization of oxidized LDL.

Sources of funding

This material is based upon work supported, in part, by the US Department of Veterans Affairs, Veterans Health Administration, Office of Research and Development, Biomedical Laboratory Research and Development. This work was supported by a Merit Review Award from the US Department of Veterans Affairs, the Flight Attendant Medical Research Institute and National Institutes of Health R01 grants HL096376, HL097376, HL098174, HL081784, 1UH2HL123502, P01HL114453 (to R.K.M.), 1K23HL126912 (to D.C.), the Samuel Winters Foundation (713263, to D.C.), and HL084948 (F.C·S). This research is also supported by ME-02-384 (Pennsylvania Department of Health, the Department specifically disclaims responsibility for any analyses, interpretations or conclusions). The contents presented do not represent the views of the Department of Veterans Affairs or the United States Government. The funding sources did not have a direct role in the design, conduct, interpretation, writing, or decision to submit this manuscript for publication.

Abbreviations

Fbx	F-box
SCF	Skip-Cullin-F box
Skp1	Skip 1
Cul1	Cullin 1
Rbx1	ring-box protein 1
IL	interleukin
TNF-α	tumor necrosis factor
TRAF	TNF receptor associated factors
TLR	Toll-like receptors
UPS	ubiquitin proteasome system
NF-κB	nuclear factor kappa B
LPS	lipopolysaccharide
OxLDL	oxidized low density lipoprotein

References

[1]. Mensah GA, Brown DW, An overview of cardiovascular disease burden in the United States, Health Aff (Millwood) 26 (1) (2007) 38–48. [PubMed: 17211012]

[2]. Back M, Hansson GK, Anti-inflammatory therapies for atherosclerosis, Nat. Rev. Cardiol 12 (4) (2015) 199–211. [PubMed: 25666404]

[3]. Ridker PM, Luscher TF, Anti-inflammatory therapies for cardiovascular disease, Eur. Heart J 35 (27) (2014) 1782–1791. [PubMed: 24864079]

[4]. Khan R, Spagnoli V, Tardif JC, L'Allier PL, Novel anti-inflammatory therapies for the treatment of atherosclerosis, Atherosclerosis 240 (2) (2015) 497–509. [PubMed: 25917947]

Author Manuscript Author Manuscript Author Manuscript Author Manuscript

[5]. Libby P, Inflammation in atherosclerosis, Nature 420 (6917) (2002) 868–874. [PubMed: 12490960]

[6]. Ridker PM, Everett BM, Thuren T, MacFadyen JG, Chang WH, Ballantyne C, Fonseca F, Nicolau J, Koenig W, Anker SD, et al., Antiinflammatory therapy with canakinumab for atherosclerotic disease, N. Engl. J. Med 377 (12) (2017) 1119–1131. [PubMed: 28845751]

[7]. Hansson GK, Inflammation and atherosclerosis - the end of a controversy, Circulation 136 (20) (11 14 2017) 1875–1877. [PubMed: 28916641]

[8]. Stewart CR, Stuart LM, Wilkinson K, van Gils JM, Deng J, Halle A, Rayner KJ, Boyer L, Zhong R, Frazier WA, et al., CD36 ligands promote sterile inflammation through assembly of a Toll-like receptor 4 and 6 heterodimer, Nat. Immunol 11 (2) (2010) 155–161. [PubMed: 20037584]

[9]. O'Neill LA, Golenbock D, Bowie AG, The history of Toll-like receptors - redefining innate immunity, Nat. Rev. Immunol 13 (6) (2013) 453–460. [PubMed: 23681101]

[10]. Chen BB, Coon TA, Glasser JR, McVerry BJ, Zhao J, Zhao Y, Zou C, Ellis B, Sciurba FC, Zhang Y, et al., A combinatorial F box protein directed pathway controls TRAF adaptor stability to regulate inflammation, Nat. Immunol 14 (5) (2013) 470–479. [PubMed: 23542741]

[11]. Muratani M, Tansey WP, How the ubiquitin-proteasome system controls transcription, Nat. Rev. Mol. Cell Biol 4 (3) (2003) 192–201. [PubMed: 12612638]

[12]. Weathington NM, Mallampalli RK, Emerging therapies targeting the ubiquitin proteasome system in cancer, J. Clin. Invest 124 (1) (2014) 6–12. [PubMed: 24382383]

[13]. Chandra D, Gupta A, Strollo PJ Jr., Fuhrman CR, Leader JK, Bon J, Slivka WA, Shoushtari AH, Avolio J, Kip KE, et al., Airflow limitation and endothelial dysfunction. Unrelated and independent predictors of atherosclerosis, Am. J. Respir. Crit. Care Med 194 (1) (2016) 38–47. [PubMed: 26771278]

[14]. Touboul PJ, Hennerici MG, Meairs S, Adams H, Amarenco P, Desvarieux M, Ebrahim S, Fatar M, Hernandez Hernandez R, Kownator S, et al., Mannheim intima-media thickness consensus, Cerebrovasc. Dis 18 (4) (2004) 346–349. [PubMed: 15523176]

[15]. Spence JD, Eliasziw M, Dicicco M, Hackam DG, Galil R, Lohmann T, Carotid plaque area: a tool for targeting and evaluating vascular preventive therapy, Stroke 33 (12) (2002) 2916–2922. [PubMed: 12468791]

[16]. Budoff MJ, Nasir K, Kinney GL, Hokanson JE, Barr RG, Steiner R, Nath H, Lopez-Garcia C, Black-Shinn J, Casaburi R, Coronary artery and thoracic calcium on noncontrast thoracic CT scans: comparison of ungated and gated examinations in patients from the COPD Gene cohort, J. Cardiovasc. Comput. Tomogr 5 (2) (2011) 113–118. [PubMed: 21167806]

[17]. Kirsch J, Buitrago I, Mohammed TL, Gao T, Asher CR, Novaro GM, Detection of coronary calcium during standard chest computed tomography correlates with multi-detector computed tomography coronary artery calcium score, Int. J. Cardiovasc. Imaging 28 (5) (2012) 1249–1256. [PubMed: 21833776]

[18]. Einstein AJ, Johnson LL, Bokhari S, Son J, Thompson RC, Bateman TM, Hayes SW, Berman DS, Agreement of visual estimation of coronary artery calcium from low-dose CT attenuation correction scans in hybrid PET/CT and SPECT/CT with standard Agatston score, J. Am. Coll. Cardiol 56 (23) (2010) 1914–1921. [PubMed: 21109114]

[19]. Kim SM, Chung MJ, Lee KS, Choe YH, Yi CA, Choe BK, Coronary calcium screening using low-dose lung cancer screening: effectiveness of MDCT with retrospective reconstruction, AJR Am. J. Roentgenol 190 (4) (2008) 917–922. [PubMed: 18356437]

[20]. Chandra D, Gupta A, Leader JK, Fitzpatrick M, Kingsley LA, Kleerup E, Haberlen SA, Budoff MJ, Witt M, Post WS, et al., Assessment of coronary artery calcium by chest CT compared with EKG-gated cardiac CT in the multicenter AIDS cohort study, PLoS ONE 12 (4) (2017) e0176557. [PubMed: 28453572]

[21]. Aldridge GM, Podrebarac DM, Greenough WT, Weiler IJ, The use of total protein stains as loading controls: an alternative to high-abundance single-protein controls in semi-quantitative immunoblotting, J. Neurosci. Methods 172 (2) (2008) 250–254. [PubMed: 18571732]

[22]. Colella AD, Chegenii N, Tea MN, Gibbins IL, Williams KA, Chataway TK, Comparison of stain-free gels with traditional immunoblot loading control methodology, Anal. Biochem 430 (2) (2012) 108–110. [PubMed: 22929699]

Author Manuscript Author Manuscript Author Manuscript Author Manuscript

[23]. Eaton SL, Roche SL, Llavero Hurtado M, Oldknow KJ, Farquharson C, Gillingwater TH, Wishart TM, Total protein analysis as a reliable loading control for quantitative fluorescent Western blotting, PLoS ONE 8 (8) (2013) e72457. [PubMed: 24023619]

[24]. Xu S, Huang Y, Xie Y, Lan T, Le K, Chen J, Chen S, Gao S, Xu X, Shen X, et al., Evaluation of foam cell formation in cultured macrophages: an improved method with Oil Red O staining and DiI-oxLDL uptake, Cytotechnology 62 (5) (2010) 473–481. [PubMed: 21076992]

[25]. Frank PG, Lee H, Park DS, Tandon NN, Scherer PE, Lisanti MP, Genetic ablation of caveolin-1 confers protection against atherosclerosis, Arterioscler. Thromb. Vasc. Biol 24 (1) (2004) 98–105. [PubMed: 14563650]

[26]. Martius G, Cameron S, Rave-Frank M, Hess CF, Wolff HA, Malik IA, The anti-TNF-alpha antibody infliximab inhibits the expression of fat-transporter-protein FAT/CD36 in a selective hepatic-radiation mouse model, Int. J. Mol. Sci 16 (3) (2015) 4682–4697. [PubMed: 25739082]

[27]. Hoosdally SJ, Andress EJ, Wooding C, Martin CA, Linton KJ, The human scavenger receptor CD36: glycosylation status and its role in trafficking and function, J. Biol. Chem 284 (24) (2009) 16277–16288. [PubMed: 19369259]

[28]. Powell SR, Herrmann J, Lerman A, Patterson C, Wang X, The ubiquitin-proteasome system and cardiovascular disease, Prog. Mol. Biol. Transl. Sci 109 (2012) 295–346. [PubMed: 22727426]

[29]. Brand K, Page S, Walli AK, Neumeier D, Baeuerle PA, Role of nuclear factor-kappa B in atherogenesis, Exp. Physiol 82 (2) (1997) 297–304. [PubMed: 9129944]

[30]. Ritchie ME, Nuclear factor-kappaB is selectively and markedly activated in humans with unstable angina pectoris, Circulation 98 (17) (1998) 1707–1713. [PubMed: 9788823]

[31]. Jawien J, Gajda M, Mateuszuk L, Olszanecki R, Jakubowski A, Szlachcic A, Korabiowska M, Korbut R, Inhibition of nuclear factor-kappaB attenuates arther-osclerosis in apoE/LDLR - double knockout mice, J. Physiol. Pharmacol 56 (3) (2005) 483–489. [PubMed: 16204769]

[32]. Rader DJ, IL-1 and atherosclerosis: a murine twist to an evolving human story, J. Clin. Invest 122 (1) (2012) 27–30. [PubMed: 22201674]

[33]. Apostolakis S, Vogiatzi K, Amanatidou V, Spandidos DA, Interleukin 8 and cardiovascular disease, Cardiovasc. Res 84 (3) (2009) 353–360. [PubMed: 19617600]

[34]. Boisvert WA, Curtiss LK, Terkeltaub RA, Interleukin-8 and its receptor CXCR2 in atherosclerosis, Immunol. Res 21 (2–3) (2000) 129–137. [PubMed: 10852110]

[35]. Branen L, Hovgaard L, Nitulescu M, Bengtsson E, Nilsson J, Jovinge S, Inhibition of tumor necrosis factor-alpha reduces atherosclerosis in apolipoprotein E knockout mice, Arterioscler. Thromb. Vasc. Biol 24 (11) (2004) 2137–2142. [PubMed: 15345516]

[36]. Boesten LS, Zadelaar AS, van Nieuwkoop A, Gijbels MJ, de Winther MP, Havekes LM, van Vlijmen BJ, Tumor necrosis factor-alpha promotes atherosclerotic lesion progression in APOE*3-Leiden transgenic mice, Cardiovasc. Res 66 (1) (2005) 179–185. [PubMed: 15769461]

[37]. Wojczynski MK, Li M, Bielak LF, Kerr KF, Reiner AP, Wong ND, Yanek LR, Qu L, White CC, Lange LA, et al., Genetics of coronary artery calcification among African Americans, a meta-analysis, BMC Med. Genet 14 (2013) 75. [PubMed: 23870195]

[38]. Herrmann J, Lerman LO, Lerman A, On to the road to degradation: atherosclerosis and the proteasome, Cardiovasc. Res 85 (2) (2010) 291–302. [PubMed: 19815565]

[39]. Willis MS, Townley-Tilson WH, Kang EY, Homeister JW, Patterson C, Sent to destroy: the ubiquitin proteasome system regulates cell signaling and protein quality control in cardiovascular development and disease, Circ. Res 106 (3) (2010) 463–478. [PubMed: 20167943]

[40]. Aleidi SM, Howe V, Sharpe LJ, Yang A, Rao G, Brown AJ, Gelissen IC, The E3 ubiquitin ligases, HUWE1 and NEDD4–1, are involved in the post-translational regulation of the ABCG1 and ABCG4 lipid transporters, J. Biol. Chem 290 (40) (2015) 24604–24613. [PubMed: 26296893]

[41]. Calkin AC, Lee SD, Kim J, Van Stijn CM, Wu XH, Lusis AJ, Hong C, Tangirala RI, Tontonoz P, Transgenic expression of dominant-active IDOL in liver causes diet-induced hypercholesterolemia and atherosclerosis in mice, Circ. Res 115 (4) (2014) 442–449. [PubMed: 24935961]

Author Manuscript Author Manuscript Author Manuscript Author Manuscript

[42]. Groulx I, Lee S, Oxygen-dependent ubiquitination and degradation of hypoxia-inducible factor requires nuclear-cytoplasmic trafficking of the von Hippel-Lindau tumor suppressor protein, Mol. Cell. Biol 22 (15) (2002) 5319–5336. [PubMed: 12101228]

[43]. Miyawaki S, Imai H, Shimizu M, Yagi S, Ono H, Mukasa A, Nakatomi H, Shimizu T, Saito N, Genetic variant RNF213 c.14576G > a in various phenotypes of intracranial major artery stenosis/occlusion, Stroke 44 (10) (2013) 2894–2897. [PubMed: 23970789]

[44]. Goru SK, Pandey A, Gaikwad AB, E3 ubiquitin ligases as novel targets for inflammatory diseases, Pharmacol. Res 106 (2016) 1–9. [PubMed: 26875639]

Author Manuscript Author Manuscript Author Manuscript Author Manuscript

A.

	Wild type	Mutant	p value
n (%)	122 (83.6)	24 (16.4)	-
Age, years	66.2 (5.3)	66.7 (5.1)	0.77
Male (%)	53.3	33.3	0.17
Body mass index, kg/m^2	28.4 (4.6)	28.3 (3.7)	0.80
Current smoker (%)	38.5	33.3	0.49
Pack years of smoking	45.3 (21.6)	53.0 (21.7)	0.06
Systolic BP, mm Hg	136.1 (17.9)	134.7 (12.8)	0.97
Diastolic BP, mm Hg	74.5 (10.2)	72.3 (5.6)	0.19
Hypertension(%)	58.2	66.7	0.36
Diabetes Mellitus (%)	10.7	8.3	0.99
Dyslipidemia (%)	56.2	54.2	0.82
ACE inhibitor use (%)	23.0	16.7	0.78
Aspirin use (%)	53.3	50.0	0.99
Stain use (%)	47.9	41.7	0.82

B.

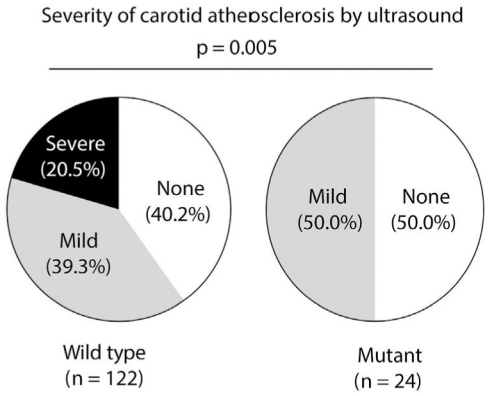

Fig. 1.

A hypofunctioning polymorphism in FBXO3 (rs1402954) is associated with less carotid atherosclerosis. A. Genomic DNA was extracted from the PBMCs of 146 individuals and used to determine if rs1402954 was absent (wild type) or present (mutant)using a specific primer and probe set. Clinical data were collected on the day of the study visit. p-values were calculated using Mann Whitney *U* test for continuous variables and Fischer's exact test for categorical variables. B. Severity of carotid atherosclerosis was assessed by carotid ultrasound by technicians blinded to FBXO3 genotype and clinical data. Individuals were classified as having none (0 plaque), mild (1–3 plaque) or severe (> 3 plaque) atherosclerosis based on ultrasound. P-value was generated using Fischer's exact test.

Author Manuscript Author Manuscript Author Manuscript Author Manuscript

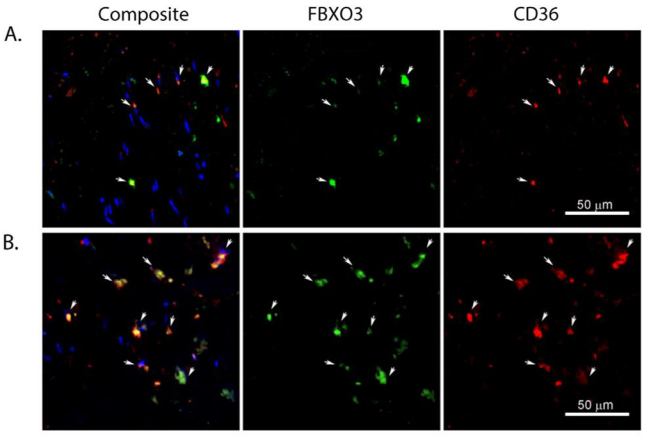

C.

	Asymptomatic	Symptomatic	p value
n	5	4	-
Age, yrs.	70.4 ± 5.3	75.0 ± 4.7	0.18
Male (%)	80.0	75.0	0.94
Ever smoker (%)	80.0	75.0	0.86
HemoglobinA1c	6.9 ± 1.1	5.7 ± 0.1	0.04
Total chol., mg/dl	168.0± 27.8	204.7 ± 108.0	0.82
LDL chol., mg/dl	96.7± 33.3	130.7 ± 91.9	0.82
HDL chol., mg/dl	28.7± 3.1	44.7 ± 14.3	0.13
Systolic BP, mg/dl	137.0 ± 18.4	164.3 ± 43.5	0.55
Diastolic BP, mg/dl	68.6 ± 4.0	80.0 ± 4.4	0.03

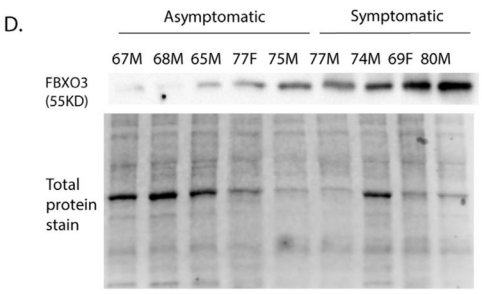

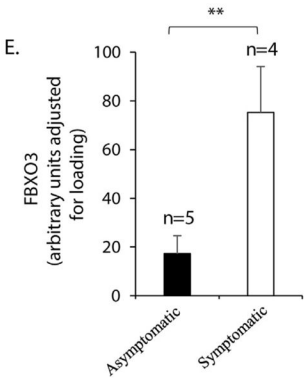

Fig. 2.

FBXO3 protein is present in carotid plaque in cells of monocytic lineage and levels are increased in symptomatic compared with asymptomatic atherosclerosis (A) Atherosclerotic plaque was surgically excised from the carotid artery of a patient with symptomatic and (B) asymptomatic carotid atherosclerosis and immunostained for DAPI (blue), FBXO3 (green), and CD68 (red). (C) Clinical data was collected by medical record review for 3 additional symptomatic patients and 4 additional asymptomatic patients. (D-E) Protein was extracted from plaque tissues of 5 patients with asymptomatic and 4 patients with symptomatic atherosclerosis, immunoblotted for FBXO3, and FBXO3 protein levelsquantified by densitometry and normalized for protein loading. Bars represent mean ± SD. p-values were calculated by Mann Whitney *U* test for continuous variables and Fischer's exact test for categorical variables. ** indicates $p < 0.001$. (For interpretation of the references to colour in this figure legend, the reader is referred to the web version of this article.)

Author Manuscript Author Manuscript Author Manuscript Author Manuscript

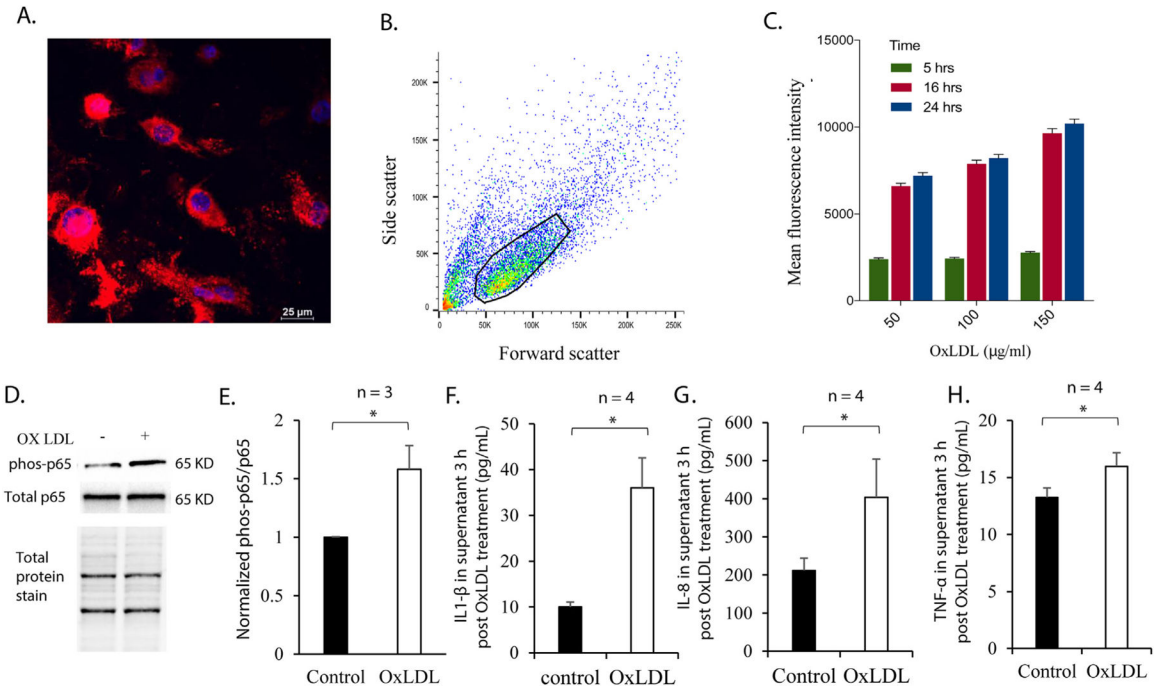

Fig. 3.

Internalization of OxLDL by THP-1 cells and inflammatory response.(A-C) THP-1 cells were matured into a macrophage phenotype using PMA, exposed to DiI-OxLDL, and imaged by confocal microscopy. Cells were also detached using trypsin, washed, and assessed by flow cytometry. Bars represent mean ± SD from > 10,000 events per condition. (D) THP-1 cells matured using PMA were exposed to OxLDL for 1 h followed by cell lysis and immunoblotting for phosphorylated and total p65. (E-F) 3 h post exposure to OxLDL supernatant from THP-1 cells was collected and cytokine levels measured by ELISA. The data in each bar graph represents the mean ± SD. p values were calculated by Mann Whitney *U* test. * indicates $p < 0.05$.

Author Manuscript Author Manuscript Author Manuscript Author Manuscript

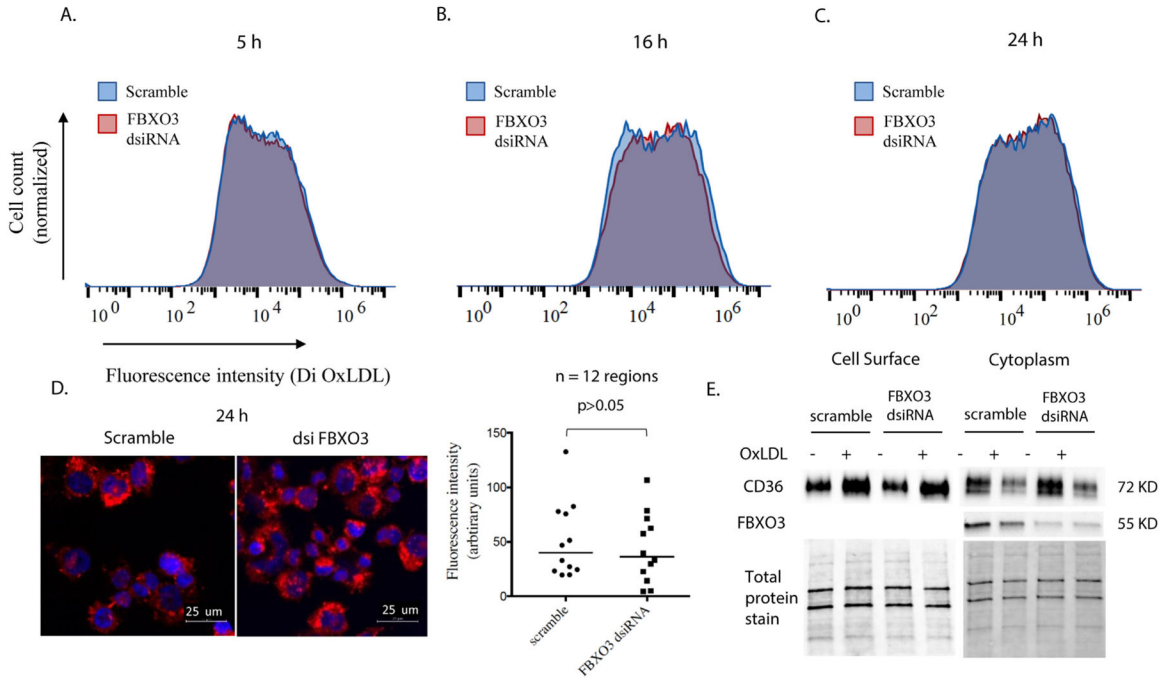

Fig. 4.

FBXO3 silencing does not impact OxLDL uptake by THP-1 cells.(A-C) Differentiated THP-1 cells were transfected with *FBXO3*or scramble dsiRNA. 48 h later the cells were incubated with 100 μg/mL Di labeled OxLDL for 5, 16, and 24 h. Cells were thendetached with trypsin. Histograms represent least 15,000 events/condition (D) To confirm flow cytometry results THP-1 cells treated as above were analyzed by confocal imaging at 24 h. The signal intensity for Di was measured using 10 μm z-stacks in 4 regions in 3 cover slips per condition. Results were normalized to the number of DAPI positive structures present in each image and p-value calculated by Mann Whitney U test. (E) Differentiated THP-1 cells were transfected with *FBXO3* vs. scramble dsiRNA. 48 h later the cells were incubated with 100 μg/mL OxLDL for 24 h. The cells were then biotinylated and the cell surface and cytoplasmic fraction immunoblotted for CD36. 24 h. The cells were then biotinylated and the cell surface and cytoplasmic fraction immunoblotted for CD36. Panel displays representative result from 3 independent experiments.

Author Manuscript Author Manuscript Author Manuscript Author Manuscript

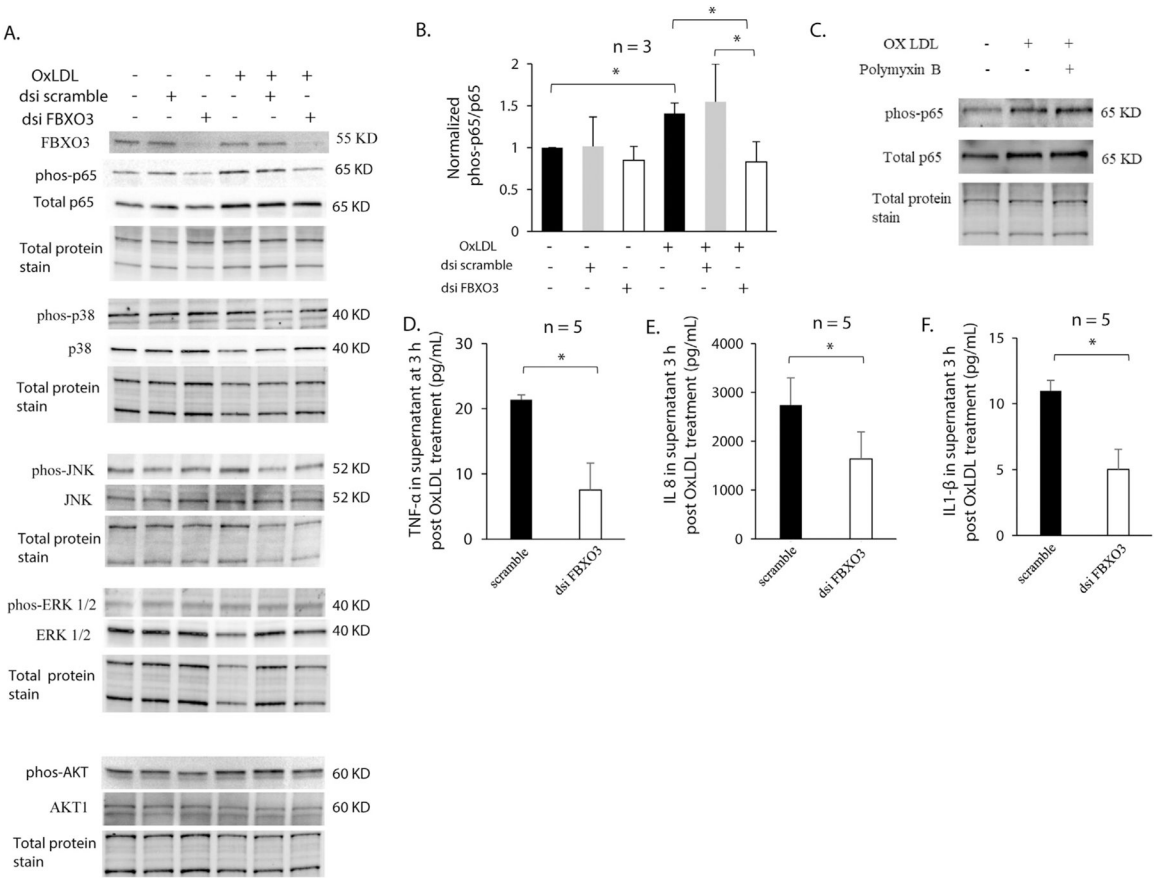

Fig. 5.

FBXO3 depletion reduces the inflammatory response to OxLDL in macrophages.(A) Differentiated THP-1 cells were mock transfected, transfected with scramble or *FBXO3*dsiRNA. 48 h later 100 μg/mL OxLDL was added to the indicated wells. 1 h later lysate was collected and immunoblotted for FBXO3, phos-p65, total p65, and MAP kinases (phos-p38, p38, phos-JNK, JNK, phosERK1/2, ERK1/2, phos-AKT, and AKT). (B) phos-p65/p65 was quantified by densitometry of panel A and in independently repeated experiments, and normalized to total protein staining with control (first lane) as the reference. (C) Differentiated THP-1 cells were untreated, or treated with 100 μg/mL OxLDL, and 100 μg/mL OxLDL that had been pre-incubated with 15 mg/mL Polymyxin B for 1 h at room temperature. Lysate was collected 1 h later and immunoblotted for phos-p65 and total p65. (D, E, F) Differentiated THP-1 cells were transfected with *FBXO3*or scramble dsiRNA. 48 h later culture medium was replaced after washing the cells twice with 1× PBS and 100 μg/mL OxLDL added. Supernatant was collected 3 h later, centrifuged at 10,000 RPM for 10 mins at 4 °C to remove particulates, and used in ELISA against IL-1β, IL-8, and TNFα. The data in each panel represents the mean ± SD and are representative of at least n = 3 independent experiments. p values were calculated by Mann Whitney U test. * indicates $p < 0.05$.

Author Manuscript
Author Manuscript
Author Manuscript
Author Manuscript

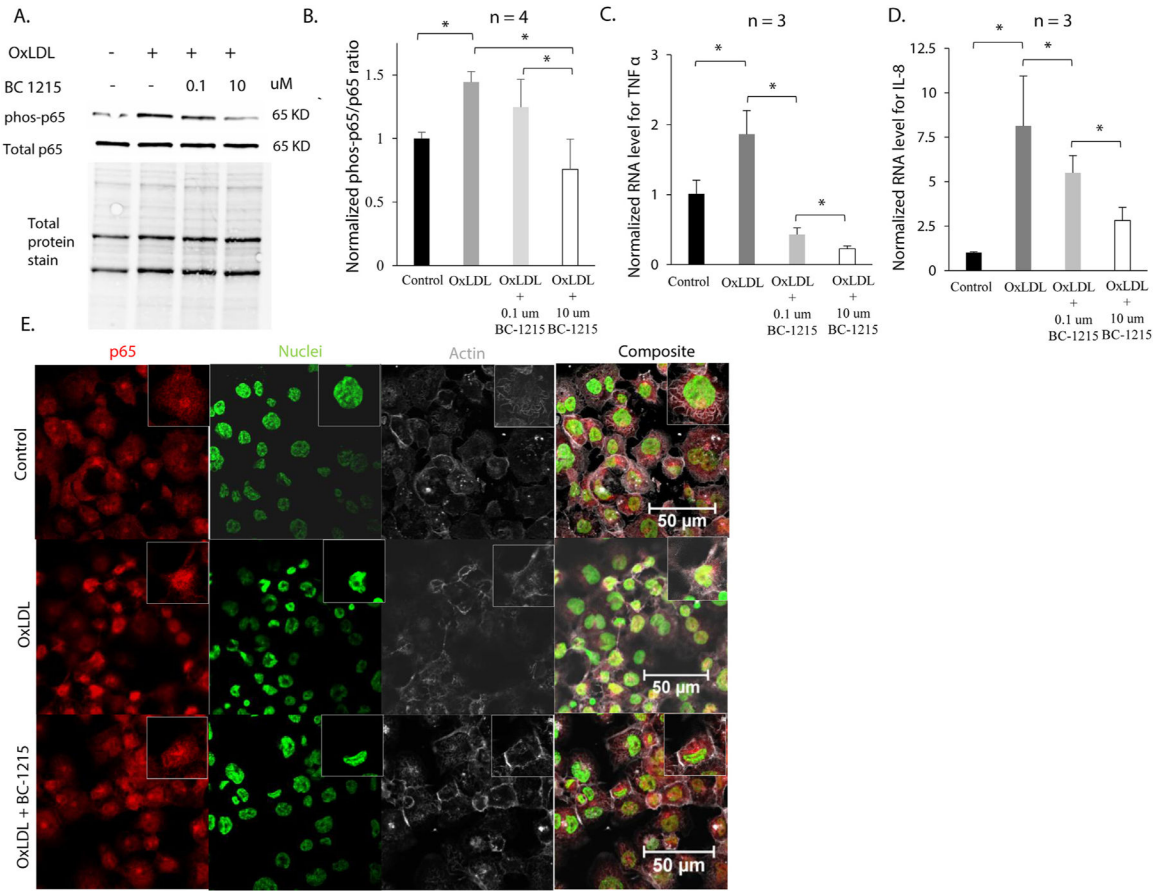

Fig. 6.

A small molecule inhibitor of FBXO3 reduces the inflammatory response to OxLDL in macrophages.(A) Differentiated THP-1 cells were incubated with BC-1215 overnight before addition of 100 µg/mL OxLDL. Cell lysate was collected 1 h later and immunoblotted for phos-p65 and total p65. (B) Phos p65/p65 was calculated by densitometry on panel A and replicate experiments. (C-D) Differentiated THP-1 cells were incubated with BC-1215 overnight before addition of 100 µg/mL OxLDL. 1 h later RNA was isolated and analyzed by RT-PCR using primers against TNF-α, IL-8, and GAPDH (for normalization). (E) Differentiated THP-1 cells were incubated with 100 µg/mL OxLDL for 90 m with and without overnight treatment with 10µM BC-1215. Cells were then fixed and stained for p65 (red), DAPI (green), phalloidin (white). (For interpretation of the references to colour in this figure legend, the reader is referred to the web version of this article.)